



Universiteit
Leiden
The Netherlands

Development of a translational model to assess the impact of opioid overdose and naloxone dosing on respiratory depression and cardiac arrest

Mann, J.; Samieegohar, M.; Chaturbedi, A.; Zirkle, J.; Han, X.M.; Ahmadi, S.F.; ... ; Li, Z.H.

Citation

Mann, J., Samieegohar, M., Chaturbedi, A., Zirkle, J., Han, X. M., Ahmadi, S. F., ... Li, Z. H. (2022). Development of a translational model to assess the impact of opioid overdose and naloxone dosing on respiratory depression and cardiac arrest. *Clinical Pharmacology & Therapeutics*, 112(5), 1020-1032. doi:10.1002/cpt.2696





Version: Publisher's Version

License: [Licensed under Article 25fa Copyright Act/Law \(Amendment Taverne\)](#)

Downloaded from: <https://hdl.handle.net/1887/3572107>

Note: To cite this publication please use the final published version (if applicable).

Development of a Translational Model to Assess the Impact of Opioid Overdose and Naloxone Dosing on Respiratory Depression and Cardiac Arrest

John Mann¹, Mohammadreza Samieegohar¹, Anik Chaturbedi¹, Joel Zirkle¹, Xiaomei Han¹, S. Farzad Ahmadi¹ , Amy Eshleman², Aaron Janowsky², Katherine Wolfrum², Tracy Swanson², Shelley Bloom², Albert Dahan³ , Erik Olofsen³, Jeffrey Florian¹, David G. Strauss¹  and Zhihua Li^{1,*} 

In response to a surge of deaths from synthetic opioid overdoses, there have been increased efforts to distribute naloxone products in community settings. Prior research has assessed the effectiveness of naloxone in the hospital setting; however, it is challenging to assess naloxone dosing regimens in the community/first-responder setting, including reversal of respiratory depression effects of fentanyl and its derivatives (fentanyls). Here, we describe the development and validation of a mechanistic model that combines opioid mu receptor binding kinetics, opioid agonist and antagonist pharmacokinetics, and human respiratory and circulatory physiology, to evaluate naloxone dosing to reverse respiratory depression. Validation supports our model, which can quantitatively predict displacement of opioids by naloxone from opioid mu receptors *in vitro*, hypoxia-induced cardiac arrest *in vivo*, and opioid-induced respiratory depression in humans from different fentanyls. After validation, overdose simulations were performed with fentanyl and carfentanil followed by administration of different intramuscular naloxone products. Carfentanil induced more cardiac arrest events and was more difficult to reverse than fentanyl. Opioid receptor binding data indicated that carfentanil has substantially slower dissociation kinetics from the opioid receptor compared with nine other fentanyls tested, which likely contributes to the difficulty in reversing carfentanil. Administration of the same dose of naloxone intramuscularly from two different naloxone products with different formulations resulted in differences in the number of virtual patients experiencing cardiac arrest. This work provides a robust framework to evaluate dosing regimens of opioid receptor antagonists to reverse opioid-induced respiratory depression, including those caused by newly emerging synthetic opioids.

Study Highlights

WHAT IS THE CURRENT KNOWLEDGE ON THE TOPIC?

☑ It is challenging to assess naloxone dosing regimens in the community/first-responder setting, including to reverse the respiratory depression effects of fentanyl and its derivatives.

WHAT QUESTION DID THIS STUDY ADDRESS?

☑ Can quantitative systems pharmacology modeling be used to evaluate naloxone dosage regimens in a quantitative and clinically meaningful manner?

WHAT DOES THIS STUDY ADD TO OUR KNOWLEDGE?

☑ This study adopted a stringent validation strategy to develop a model that translates *in vitro* receptor binding kinetics into

clinical outcomes of opioid-induced respiratory depression, such as cardiac arrest. Initial modeling suggests respiratory depression induced by carfentanil is difficult to reverse due to its slow dissociation kinetics from the opioid receptor and a naloxone product's formulation can impact naloxone's ability to prevent cardiac arrest.

HOW MIGHT THIS CHANGE CLINICAL PHARMACOLOGY AND THERAPEUTICS?

☑ This work presents a robust framework for assessing the ability of naloxone formulations and dosing to reverse opioid overdose in a community setting, including for newly emerging synthetic opioids with little clinical data.

¹Division of Applied Regulatory Science, Office of Clinical Pharmacology, Office of Translational Sciences, Center for Drug Evaluation and Research, US Food and Drug Administration, Silver Spring, Maryland, USA; ²Department of Veteran's Affairs, Portland Health Care System, Portland, Oregon, USA; ³Leiden University Medical Center, Leiden, The Netherlands. *Correspondence: Zhihua Li (zhihua.li@fda.hhs.gov)

Received April 20, 2022; accepted June 12, 2022. doi:10.1002/cpt.2696

An increasing number of opioid-related deaths^{1,2} are attributed to synthetic opioids, such as fentanyl and its derivatives.^{3,4} As part of the strategy to combat the opioid crisis, naloxone, a fast-acting opioid mu receptor antagonist capable of reversing opioid-induced toxicity, has been distributed and utilized in the community and pre-hospital settings.⁵ The American Heart Association has provided dosing recommendations in the community setting⁶ and the US Food and Drug Administration (FDA) has approved intramuscular autoinjector and intranasal naloxone products that can be used by lay persons in the community.^{7,8} However, data to evaluate naloxone dosing in the community setting are limited.

In 2016, the FDA held a joint meeting of the Anesthetic and Analgesic Drug Products Advisory Committee and the Drug Safety and Risk Management Advisory Committee wherein some discussion focused on naloxone dosing for community use. Although there was general agreement that the risk of under-dosing naloxone far outweighs the potential risk of precipitating opioid withdrawal, a consensus could not be reached on certain aspects due to a lack of evidence supporting a specific dosing recommendation.⁹

It is difficult to recommend specific naloxone dose requirements for overdose scenarios because the necessary naloxone amount depends on the amount of opioid, the pharmacokinetics of the opioid and naloxone, and the kinetic interactions between the opioid and naloxone at the opioid mu receptor (referred to as opioid receptor throughout).⁵ For example, pharmacokinetic-pharmacodynamic modeling demonstrated that the difficulty in reversing buprenorphine-induced respiratory depression is linked to its slow dissociation kinetics from the opioid receptor.¹⁰

Furthermore, with the continued emergence of new illicitly manufactured synthetic opioids, in particular fentanyl derivatives, evaluating if such compounds have similar slow dissociation kinetics that may require more aggressive naloxone dosing is valuable.

In the present study, we report on the development and validation of a model that integrates the: (i) pharmacokinetics of opioid receptor agonists and antagonists, (ii) opioid receptor binding kinetics of agonists and antagonists, (iii) impact of opioid receptor binding on ventilation, and (iv) physiological effects of changes in ventilation on oxygen and carbon dioxide gas exchange in the lungs and circulation to the body, in particular the brain, and the subsequent feedback to ventilation (Figure 1). Compared with prior models, we enhanced the physiological component to reflect the initial compensatory increase in cardiac output following acute severe hypoxemia that subsequently decompensates leading to cardiac arrest if adequate respiration is not provided.

METHODS

Detailed methods are provided in the [Supplementary Document](#), which are summarized here.

In vitro receptor binding experiments

Fentanyl and nine of its derivatives (carfentanil, sufentanil, butyryl fentanyl, 4-fluorobutyrylfentanyl, 4-fluoroisobutyryl fentanyl, furanyl fentanyl, isobutyryl fentanyl, alfentanil, and remifentanyl), as well as buprenorphine and naloxone were radiolabeled with [³H] and used in association or dissociation assays. The same set of binding parameters (e.g., K_{on} , K_{off} , n , see [Supplementary Methods](#) for details) were derived to fit

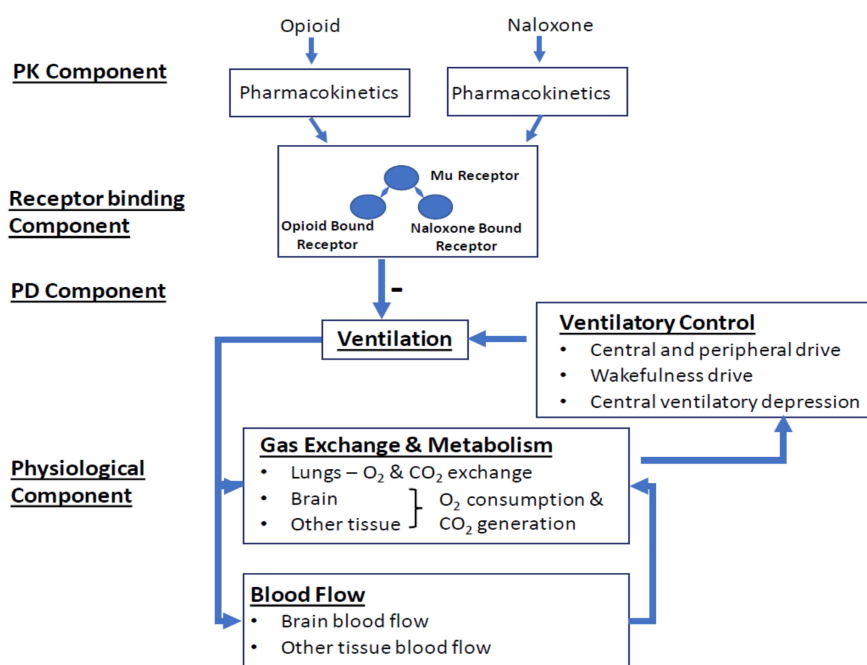


Figure 1 Overall structure of the model. The model has four components. In the pharmacokinetic (PK) component, compartment PK models convert the doses of opioids and naloxone through different dosing routes to their free concentrations in the effective compartment. In the receptor binding component, opioid and naloxone compete to bind to the opioid receptor. In the pharmacodynamic (PD) component, the opioid-bound receptors, but not the naloxone-bound receptors, lead to respiratory depression, through reducing all three ventilatory drives (central chemoreflex, peripheral chemoreflex, and wakefulness drives). The physiological component describes gas (oxygen (O₂) and carbon dioxide (CO₂)) exchange and metabolism, ventilatory control, and blood flow control. [Colour figure can be viewed at [wileyonlinelibrary.com](#)]

all association and dissociation experiments for the same ligand (opioid or naloxone).

Model development procedures

To increase the credibility of the final model predictions, we designed a model development strategy that involved a model calibration phase and a model validation phase.

Model calibration

In the model calibration phase, the receptor binding, pharmacokinetic, physiology, and pharmacodynamic submodels were built and parameterized based on new *in vitro* binding experiments (see [Supplementary Methods](#)) and existing pharmacokinetic and physiology data.

Some pharmacokinetic submodels and parameter sets were taken directly from the literature, such as intravenous administration of fentanyl¹¹ and remifentanyl.¹² For carfentanyl, the only available clinical study with intravenous administration¹³ did not report plasma concentrations, but rather reported a long plasma half-life (~45 minutes) after bolus injections. Accordingly, for the carfentanyl model, we modified the fentanyl pharmacokinetic model to fit this half-life (see [Supplementary Materials](#)). For the pharmacokinetics of naloxone following intramuscular administration, plasma concentration profiles of two intramuscular formulations (generic naloxone hydrochloride injection 2 mg/2 mL¹⁴ and naloxone hydrochloride injection with autoinjector 2 mg/0.4 mL¹⁵) were used to construct the structural pharmacokinetic model for each product. Both naloxone products share the same pharmacokinetic model structure with two transit, one central, and one peripheral compartment.

The physiology submodel was based on a previous model developed by Ursino *et al.*^{16,17} that was calibrated using clinical data of ventilatory response under various conditions, such as iso-oxic hypercapnia, hyperoxia and normocapnia, iso-capnic hypoxia, and poikilocapnic hypoxia. We updated the original model to better reproduce various clinical data and expanded the model to capture changes in total systemic blood flow (cardiac output) and cerebral blood flow that occur following acute severe hypoxia.^{18–20} In the model, we defined cardiac arrest as total blood flow reduced to 0.01 L/min, which most commonly corresponds to pulseless electrical activity progressing to asystole in patients with opioid-induced out-of-hospital cardiac arrest.²¹

The pharmacodynamic submodel was calibrated based on two clinical studies investigating the impact of fentanyl on ventilation.^{11,22} To visually compare the model simulation and clinical data, a population model was constructed to capture intersubject variability and model parameter uncertainty. Randomly sampled pharmacokinetic parameters based on the population pharmacokinetic models ([Table S1](#)) were combined with estimated distributions of receptor binding parameters ([Table S2](#)) to form a population of 2,000 virtual patients for population simulations.

Model validation

In the subsequent validation phase, various components of the model were “frozen” and used to predict new data not used during model calibration. This included *in vitro* opioid-naloxone competitive assays, animal studies with severe hypoxia-induced cardiac arrest,²⁰ and clinical ventilation studies with fentanyl, alfentanil, and remifentanyl.^{23,24} Although there is no universally accepted predictive performance criteria for quantitative systems pharmacology models, the fields of other mechanistic models, such as physiologically-based pharmacokinetic models, commonly use a twofold deviation (predicted value within 0.5 times to 2 times of the observed value) as a performance criterion.²⁵ Accordingly, we calculated the ratio between the mean model-predicted value (prediction using typical parameters) and the mean observed value in the validation data sets to evaluate our model’s predictive credibility. In addition, the 95% confidence intervals of the population model predictions were plotted against clinical data to assess for similar trends.

Opioid overdose simulations

The opioid overdose scenarios were based on real-world data from a study of ~500 fatal fentanyl overdose cases.²⁶ We estimated the “medium” and “high” intravenous doses to be 1.63 and 2.97 mg, respectively ([Supplementary Methods](#)). As there are limited fatal overdose data available for carfentanyl, we utilized a dose equivalence strategy to calculate its medium and high overdose scenarios. With this strategy, the minimum dose required to induce cardiac arrest was calculated for both fentanyl and carfentanyl. The ratio of these minimum doses (carfentanyl/fentanyl) was multiplied by the medium and high fentanyl doses to derive the corresponding medium and high overdose scenarios for carfentanyl of 0.012 and 0.022 mg, respectively.

To simulate naloxone reversal of opioid-induced respiratory depression, we needed to define the ventilation threshold to trigger naloxone administration. A threshold of 40% of baseline minute ventilation was selected based on review of naloxone training materials and animal studies (see [Supplementary Methods](#) for detailed rationale). The same threshold was used by others²⁷ as an unsafe level of respiration induced by opioids. At each dose, we simulated virtual patients where opioid was administered via intravenous injection, and pharmacokinetic/pharmacodynamic outputs were calculated continuously for 1.5 hours. We simulated intramuscular naloxone administration 1 minute after ventilation decreased to 40% of baseline to mimic a delay between recognizing respiratory depression and administering naloxone.

Both the typical virtual patient (the model with typical parameters) and virtual populations were simulated to compare different opioid overdose and naloxone dosing scenarios. Code for overdose simulations can be found in <https://github.com/FDA/Mechanistic-PK-PD-Model-to-Rescue-Opioid-Overdose>.

RESULTS

Model calibration

[Figure 1](#) shows the overall model structure. It is comprised of the receptor binding component (submodel) to simulate opioid vs. naloxone competition on the opioid receptor; the pharmacokinetic component to link drug dose to clinical exposure through different dosing routes; the physiological component describing gas (oxygen and carbon dioxide) metabolism and exchange, ventilatory control, as well as blood flow control; and the pharmacodynamic component to link the fraction of opioid receptor bound by opioids to ventilation drive. The mathematical equations and parameters for different components were estimated separately based on different data sources in the model calibration step.

For the receptor binding submodel, binding kinetic parameters for each of the ligands (opioids or naloxone) were estimated by fitting the receptor binding equations to the association and dissociation experiments for each ligand ([Figures S1 and S2](#)). These fitted parameters for all ligands are shown in [Table S2](#). Buprenorphine had the slowest dissociation kinetics (dissociation half-life 84.4 minutes), followed by carfentanyl (dissociation half-life 46.6 minutes). Sufentanyl (10.7 minutes) and remifentanyl (5.6 minutes) had the next slowest dissociation half-lives from the opioid receptor. All other opioids tested, including fentanyl and its other derivatives (alfentanil, butyryl fentanyl, fluorobutyryl fentanyl, isobutyryl fentanyl, furanyl fentanyl, and fluoroisobutyryl fentanyl), had dissociation half-lives < 3 minutes.

For the pharmacokinetic submodels, the pharmacokinetic model from Algera *et al.*^{28,29} was used for fentanyl. For naloxone administered via intramuscular injection, we developed pharmacokinetic models based on plasma profiles of generic naloxone

hydrochloride injection (2 mg/2 mL) and a more concentrated naloxone product (2 mg/0.4 mL) approved for use with an auto-injector (Figure S3).¹⁵ Table S1 contains the fitted parameters for fentanyl and naloxone.

The physiological component was updated from the model developed by Ursino *et al.*^{16,17,30} Our implementation reproduced clinical data covering human ventilation responses to different levels of hypoxia and hypercapnia, as shown by the original Ursino *et al.* model,^{16,17} and better reproduced additional clinical data. For example, our model reproduced the ventilatory change in response to a hypercapnic stimulus (end-tidal carbon dioxide elevated to ~48 mmHg) for constant hyperoxia, normoxia, and hypoxia (end-tidal oxygen fixed at 200, 100, and 53 mmHg, respectively) observed clinically, and fixed an issue with the original model leading to zero baseline minute ventilation under hyperoxic conditions¹⁶ (Figure S4). For cerebral blood flow regulation, our model reproduced clinically observed cerebral blood flow change in response to change of the partial pressure of arterial carbon dioxide, and simultaneous changes in PaCO₂ and the partial pressure of arterial oxygen, whereas the original Ursino *et al.* model did not reproduce these changes (Figure 2). For a complete description of

calibration of the physiology component, see Figures S4–S8 and Supplementary Methods.

In addition, we extended the blood flow control mechanisms in the model to link respiratory depression and cardiac arrest based on animal data (see Methods).^{18,19} Our model reproduced the initial compensatory increase in systemic and brain blood flow, subsequent decompensation, and eventual cardiac arrest induced by severe hypoxia (Figure 3).

The pharmacodynamic submodel parameters were estimated using two human studies involving fentanyl: one study where healthy opioid naïve participants were given a bolus intravenous injection of fentanyl while breathing room air,²² and another study where healthy opioid naïve participants and chronic opioid user participants were given intravenous fentanyl over 90 seconds in escalating amounts while end-tidal partial pressure of carbon dioxide was fixed at ~50 mmHg.¹¹ Our model reproduced the changes in minute ventilation and arterial oxygen and carbon dioxide levels as well as the reduction and recovery of the ventilatory response to hypercapnia in these studies (Figure 4). Notably, the simulated chronic opioid users demonstrated a similar degree of respiratory depression at a higher fentanyl dose compared with simulated

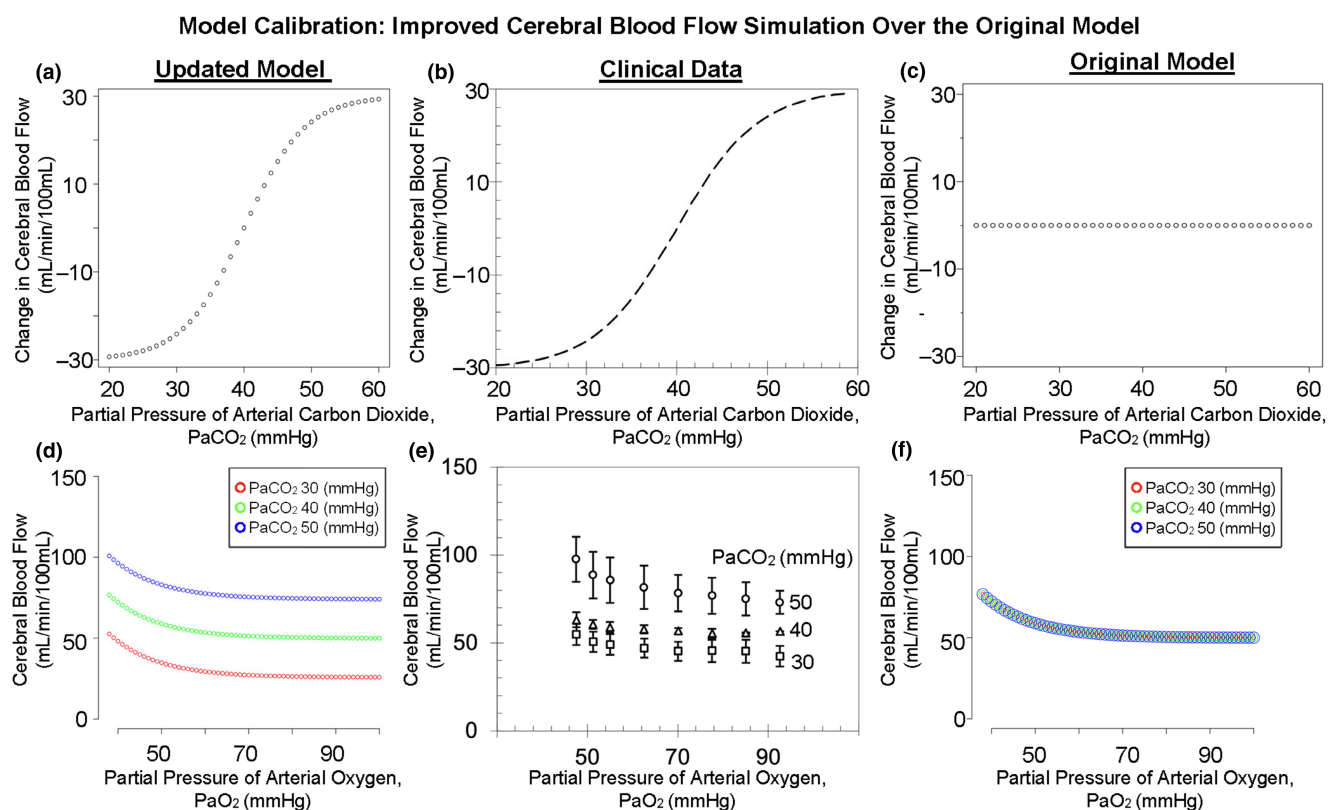


Figure 2 Cerebral blood flow changes in response to changes in carbon dioxide (top row) and simultaneous changes in oxygen and carbon dioxide (bottom row). (a) Our model simulation (updated from Ursino *et al.* model) of the relationship between arterial carbon dioxide partial pressure (PaCO₂) and the change in cerebral blood flow from baseline. (b) Clinically derived relationship.^{48,49} (c) The original simulations from the Ursino *et al.* model. It is apparent that the original Ursino *et al.* model did not capture the relationship between cerebral blood flow and arterial carbon dioxide level. (d) Our model simulation (updated from the Ursino *et al.* model) of cerebral blood flow changes in response to simultaneous changes of PaCO₂ and the partial pressure of arterial oxygen (PaO₂). (e) Clinical data.^{48,50} (f) The original simulations from the Ursino *et al.* model. Note that in the original model simulation, the three curves of cerebral blood flow vs. PaO₂ at different PaCO₂ levels completely overlap, which is not consistent with the clinical data.

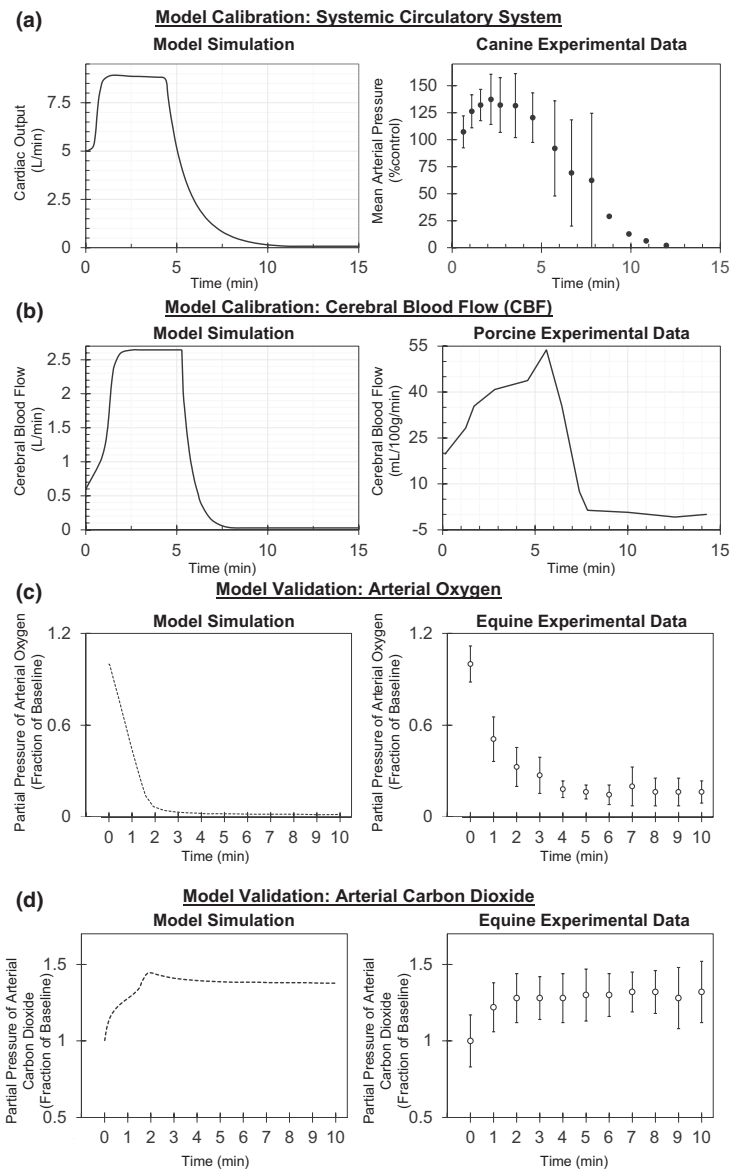


Figure 3 Calibration and validation of the cardiac arrest mechanism in the physiological submodel. The first two rows (**a**, **b**) compare model simulations (left panels) to animal data (right panels) used to calibrate the model, whereas the third and fourth rows (**c**, **d**) compare model predictions (left panel) to independent animal data (right panel) as model validation. (**a**) Left: Model simulation of human cardiac output (total blood flow) with 0.5% inspired oxygen. Right: Canine mean arterial blood pressure¹⁸ with 0.5–1% inspired oxygen. Although the end points are different between the model simulation (cardiac output) and animal data (mean arterial pressure), they both reflect the systemic circulatory system and the model reproduced the time course of the initial compensation followed by decompensation leading to cardiac arrest. (**b**) Left: Model simulation of human brain blood flow during apnea. Right: Porcine data¹⁹ showing the rise and fall of cerebral blood flow in an experimental model of fentanyl overdose with endotracheal tube clamping. Although the units are different between the model (L/min) and the animal data (mL/100g tissue/min), the model reproduced the time course of the initial compensatory increase in cerebral blood flow followed by subsequent decompensation. Of note, the experimental model in **b** involved hypoxia plus hypercapnia, whereas the experimental model in **a** only involved hypoxia. The model was able to reproduce the faster decompensation with hypoxia plus hypercapnia compared to hypoxia alone. (**c**, **d**) Model prediction of the partial pressure of arterial oxygen **c** and carbon dioxide **d** after the onset of apnea (time 0 on X axis) as compared with equine data (median and range).²⁰ Despite the species difference, the time course of changes in the partial pressure of arterial oxygen and carbon dioxide were comparable. Of note, **c** and **d** were considered model validation because model equations and parameters were not adjusted based on the equine data. [Corrections added on 23 September 2022, after first online publication: Resolution of Figure 3 has been corrected.]

healthy opioid naïve individuals at a lower dose, consistent with the clinical observations (Figure 4e,f).

Model validation

To evaluate the reliability of the model and its parameters, different model components (submodels) went through independent

validation where the model equations and parameters were “frozen” and used to predict new experimental data not used during model calibration. For the receptor binding component, the submodel was used to predict the fraction of opioid-bound receptor at equilibrium with increasing concentrations of naloxone. As shown in Figure 5, for all opioids, the predicted opioid-bound receptor profiles (shaded

PD Calibration Study 1: Fentanyl Bolus Injection while Breathing Room Air or Rebreathing

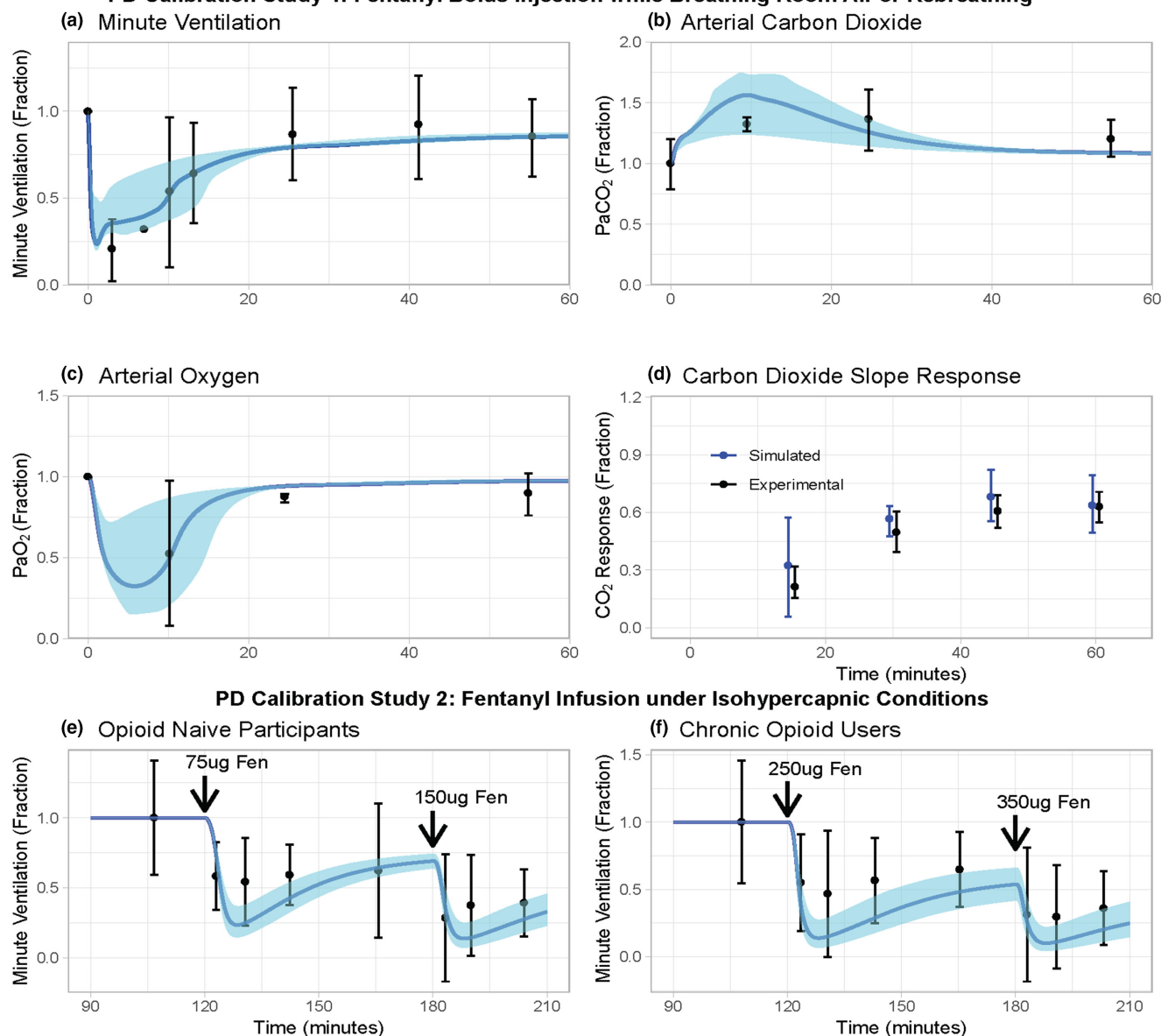


Figure 4 Calibration of the pharmacodynamic component of the model. The pharmacodynamic component describes the drug effects on the ventilatory drives, and subsequently on the partial pressures of arterial oxygen (PaO_2) and carbon dioxide (PaCO_2). (a) Minute ventilation (fraction of baseline), (b) PaCO_2 (fraction of baseline), and (c) PaO_2 (fraction of baseline) after 0.5 mg fentanyl bolus injection while study participants breathed room air.²² (d) The ventilatory response to hypercapnia (i.e., the slope of ventilation vs. end-tidal carbon dioxide response curve, expressed as a fraction of the baseline slope) was assessed through a rebreathing procedure in the same participants as displayed in panels a through c. (e, f) Minute ventilation (fraction of baseline) changes after bolus fentanyl injection for healthy opioid naïve participants e and chronic opioid user participants f with their end-tidal carbon dioxide fixed at ~50 mmHg (isohypercapnic condition).¹¹ At the 120th minute (X axis), opioid naïve and chronic opioid user participants received a bolus injection of 75 and 250 μg fentanyl/70 kg body weight, respectively. At the 180th minute (X axis), opioid naïve and chronic opioid user participants received a fentanyl intravenous injection of 150 and 350 μg /70 kg body weight, respectively. Of note, some participants received more than two doses of fentanyl; however, these higher dosing groups excluded some participants due to adverse events or fentanyl intolerance. These dosing groups with excluded subjects were not used in model calibration. Solid blue lines and bands are the typical patient (the virtual patient with typical parameters) and the 95% confidence interval (CI) of the virtual population simulations, respectively. Black dots and error bars are the mean and 95% CI of the clinical data, respectively. [Colour figure can be viewed at wileyonlinelibrary.com]

bands) followed the trend of the experimentally observed values (error bars). The median ratio between predicted and measured opioid-bound receptor fractions was 1.00 (interquartile range, 0.86–1.00).

For the physiological component, the submodel was used to predict the changes in arterial oxygen and carbon dioxide partial pressures with severe hypoxia leading to cardiac arrest in an equine study.²⁰ The model predicted the time course of changes

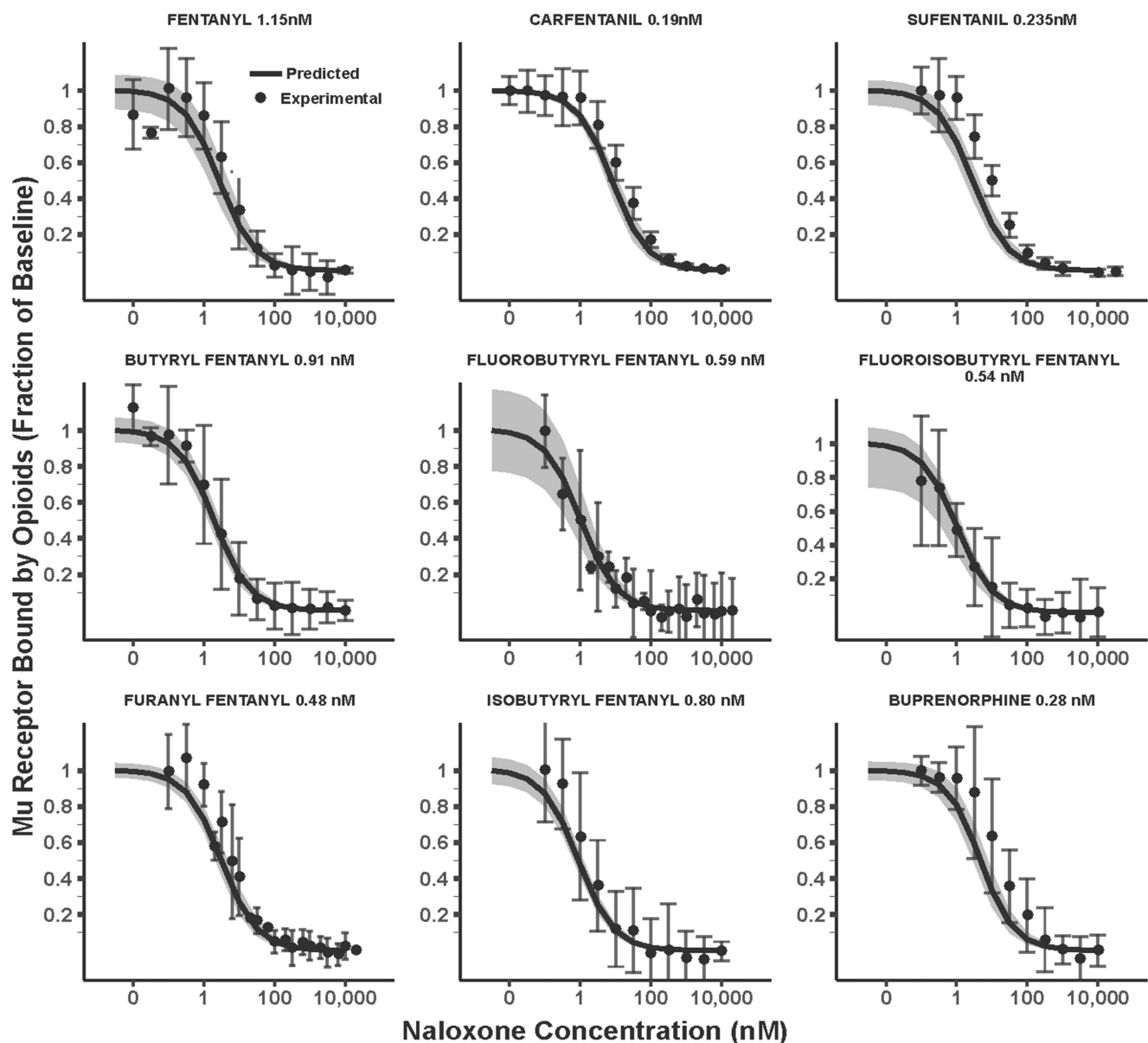


Figure 5 Independent validation of the receptor binding component using competition assays between naloxone and nine of the opioids tested. In each assay, increasing naloxone concentration (X axis) was incubated with a fixed concentration of each opioid (top of each plot) to compete for binding to the opioid receptor. The dots (mean) and error bars (95% confidence interval) correspond to the measured fraction of opioid-bound receptors from the competition assays. Solid lines and gray bands indicate the point estimate and 95% confidence interval for the predicted fraction of opioid-bound receptors in the competition assays using parameters previously derived from association/dissociation experiments (Table S2). Of note, alfentanil and remifentanil competition assay data are not available.

from baseline in arterial oxygen (Figure 3c) and carbon dioxide (Figure 3d). The median ratio between predicted and measured values was 1.00 (interquartile range, 0.92–1.06).

For the validation of the pharmacodynamic submodel, we used the model to independently predict the outcome of clinical studies. This included Mildh *et al.*²³ with computer-driven continuous infusion of fentanyl or alfentanil while study participants breathed room air (Figure 6a–f), and Olofsen *et al.*²⁴ with remifentanil infusion without fixing end-tidal carbon dioxide (Figure 6g). Of all the observed data, which included minute ventilation, arterial oxygen levels, and arterial carbon dioxide levels, the median ratio between predicted and measured values was 0.95 (interquartile range, 0.90–1.01).

Preliminary simulation of opioid overdose and naloxone administration in a community setting

Having validated the full model, we simulated chronic opioid users (see Figure 4f) under fentanyl or carfentanil overdose scenarios with or without administration of two naloxone intramuscular formulations: intramuscular 2 mg/0.4 mL¹⁵ and intramuscular 2 mg/2 mL.¹⁴

Without naloxone administration, opioid-induced decrease in ventilation led to a decrease in arterial oxygen partial pressure (red lines in Figure 7a, top two rows). The resulting acute hypoxemia initially caused a compensatory increase in cardiac output, followed by subsequent decompensation (red lines in

PD Validation Study 1: Breathing Room Air with Computer Controlled Steady State Plasma Concentration

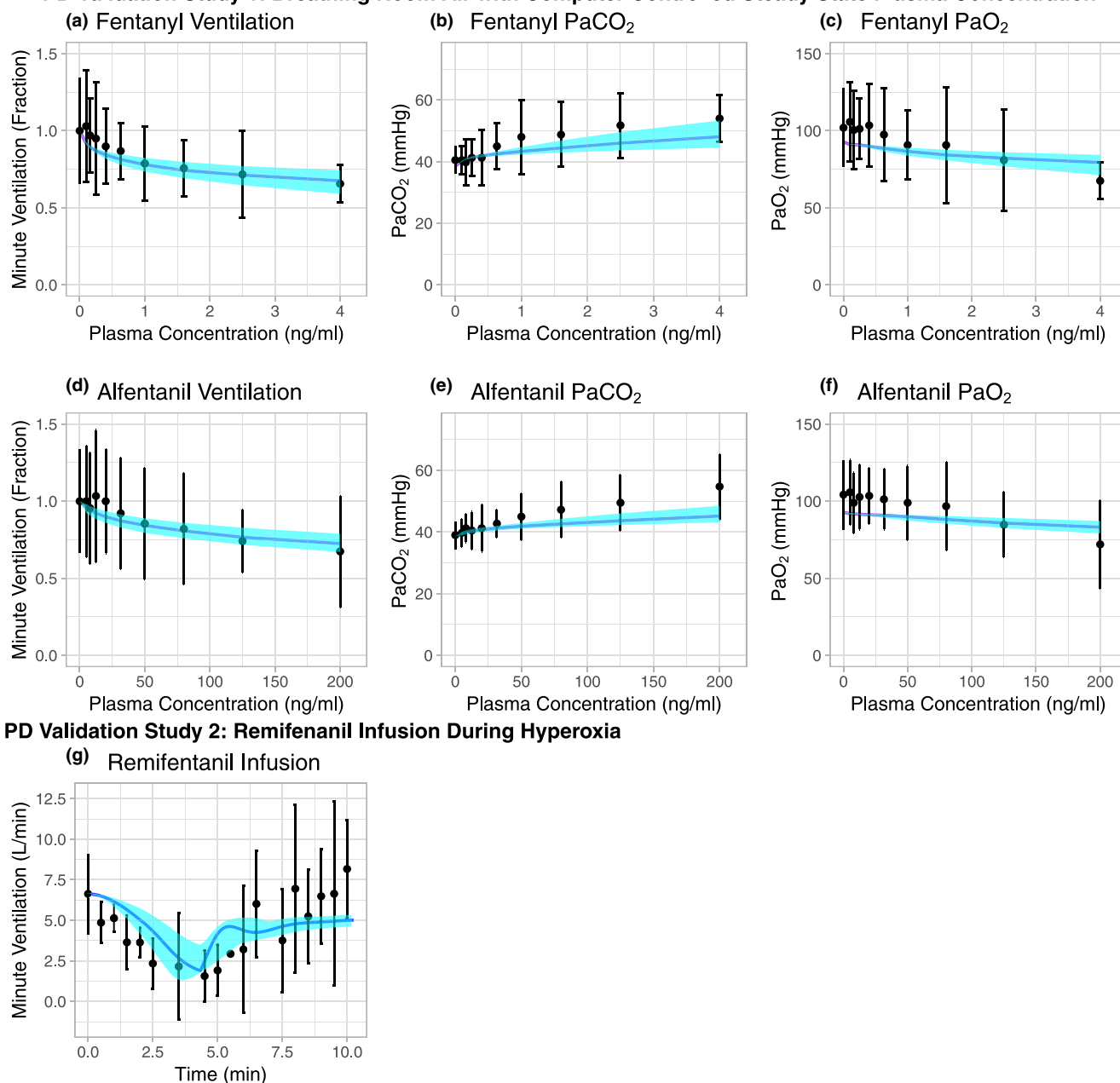
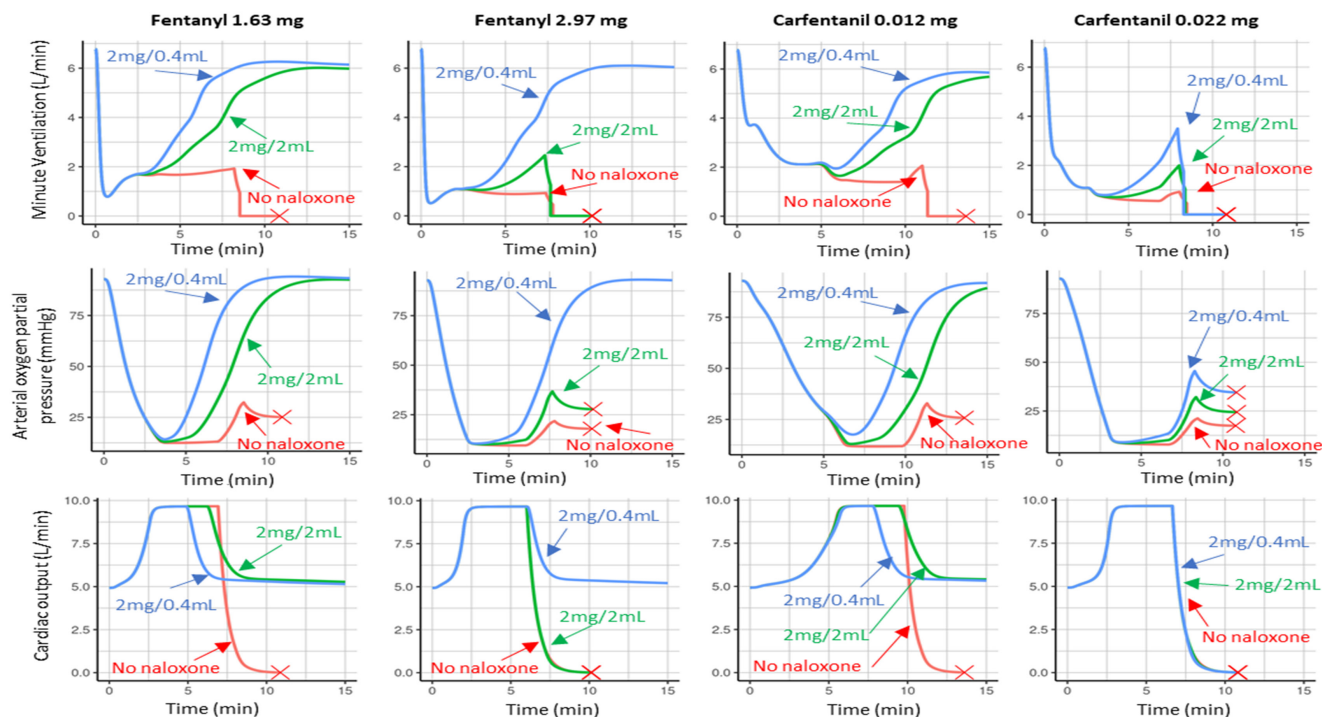


Figure 6 Validation of the pharmacodynamic (PD) component of the model. The model was “frozen” without any changes and used to predict clinical outcome from studies not used for model calibration. **(a)** Minute ventilation, **(b)** partial pressure of arterial carbon dioxide (PaCO₂), and **(c)** partial pressure of arterial oxygen (PaO₂) after computer-driven continuous fentanyl infusion to achieve various pseudo-steady-state plasma concentrations while study participants breathed room air.²³ **(d–f)** The same study with various pseudo-steady-state plasma concentrations of alfentanil. For each plasma concentration for fentanyl and alfentanil, a computer-driven infusion pump was used to maintain the desired concentration level for 10 minutes, with PD variables (ventilation, arterial gas levels, etc.) measured at 7–9 minutes, when the plasma concentration was at pseudo steady-state.²³ To mimic this design, we fixed opioid concentrations at each desired level in the model, without executing the pharmacokinetic submodel. Note that for panels **a** and **d**, the minute ventilation comparison was based on fraction of baseline instead of absolute values, because the clinical data had substantially different baseline mean minute ventilation (~10 L/min) compared with the model (6.67 L/min). Of note this study only enrolled male participants in their 20s,²³ which may explain why their baseline minute ventilation was higher than that of the general population (5–8 L/min).⁵¹ **(g)** A study²⁴ where remifentanil was administered as a continuous pump-driven infusion over 3 minutes under hyperoxic conditions. The simulated infusion scheme was adjusted to match the measured plasma concentrations (**Figure S10**). Black points and error bars are the mean and 95% confidence interval (CI) of clinically measured minute ventilation. The blue line and band are the predicted minute ventilation from the typical virtual patient and 95% CI of the virtual population, respectively. [Corrections added on 23 September 2022, after first online publication: Resolution of Figure 6 has been corrected.] [Colour figure can be viewed at [wileyonlinelibrary.com](https://onlinelibrary.wiley.com/doi/10.1002/cpt.2696)]

(a) Simulation of a Typical Patient



(b) Simulation of a Patient Population

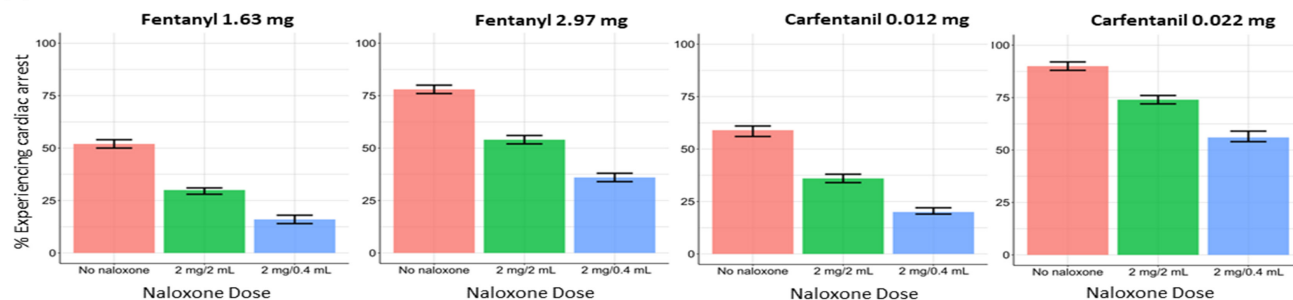


Figure 7 Model-predicted physiology and outcomes after fentanyl and carfentanil overdose in chronic opioids users and dosing evaluation for two intramuscular naloxone products. The opioid overdose scenarios tested were intravenous bolus administration of fentanyl medium overdose (1.63mg, column 1), fentanyl high overdose (2.97 mg, column 2), carfentanil medium overdose (0.012mg, column 3), and carfentanil high overdose (0.022 mg, column 4). See the [Methods](#) section for the rationale for specific opioid doses. In all graphs, no naloxone is red, generic naloxone hydrochloride injection 2 mg/2 mL is green, and naloxone hydrochloride injection with autoinjector 2 mg/0.4 mL is blue. (a) Physiological outcomes over 15 minutes from the typical virtual patient are plotted: minute ventilation (first row), partial pressure of arterial oxygen (second row), and cardiac output (third row). The red X indicates the time of cardiac arrest (defined as cardiac output reduced to 0.01 L/min; see the [Methods](#) section). Note that some cardiac output curves and red Xs from different naloxone dosing groups overlap with each other. (b) The percentage of virtual patients experiencing cardiac arrest. The error bars represent the median and interquartile range of cardiac arrest percentage after randomly sampling 200 out of the 2,000 virtual patients 2,500 times.

Figure 7a, third row) and ultimately cardiac arrest (red X in **Figure 7a**). The onset of ventilatory depression was slower for carfentanil than fentanyl (**Figure 7a**, first row), consistent with carfentanil binding to the opioid receptor more slowly (slower association rate; [Table S2](#)). As a result of the slower initial decline in ventilation with carfentanil compared with fentanyl, by the time ventilation decreased to 40% of baseline (the trigger for administering naloxone 1 minute later), carfentanil virtual patients had lower arterial oxygen and higher arterial carbon dioxide.

Naloxone administration led to a reversal of ventilatory depression (green and blue lines in **Figure 7a**, first row), an increase

of arterial oxygen partial pressure (**Figure 7a**, second row), and a return of cardiac output to baseline without cardiac arrest in some cases (**Figure 7a**, third row). For a typical virtual patient, the 2 mg/0.4 mL naloxone formulation, but not the 2 mg/2 mL formulation, rescued the high fentanyl overdose scenario (**Figure 7a**, second column) due to the more concentrated formulation having a faster rise of naloxone plasma concentration (**Figure S11**). However, with high-dose carfentanil (0.022 mg), one dose of either naloxone formulation did not reverse ventilatory depression fast enough to prevent cardiac arrest (**Figure 7a**, fourth column), consistent with a slower dissociation rate for carfentanil from the opioid receptor ([Table S2](#)). The rescue

pattern observed with the typical virtual patient simulation above was consistent with population simulations (**Figure 7b**) considering interindividual variability in pharmacokinetic and receptor binding parameters. The 2 mg/0.4 mL naloxone formulation was associated with a lower cardiac arrest percentage compared with the 2 mg/2 mL formulation. For example, for the medium fentanyl overdose of 1.63 mg, administering the 2 naloxone formulations resulted in a cardiac arrest percentage of 16% (interquartile range, 14–17%) and 30% (interquartile range, 28–31%), respectively. Carfentanil overdose, compared with fentanyl overdose, resulted in a higher percentage of cardiac arrest. For example, with the 2 mg/0.4 mL naloxone formulation, the carfentanil medium overdose (0.012 mg) resulted in 20% (interquartile range, 19–22%) cardiac arrest percentage in the virtual population, compared with 16% (interquartile range, 14–17%) with the fentanyl medium overdose (1.625 mg). The same pattern was observed with the other naloxone formulation and the higher doses of fentanyl and carfentanil (**Figure 7b**).

DISCUSSION

Here, we presented the development and validation of a model that can be used to evaluate the impact of different dosing schemes of opioid antagonists on reversing opioid-induced respiratory depression in the community setting. Compared with other similar modeling studies,³¹ we adopted a more vigorous model validation strategy by using independent *in vitro*, *in vivo*, and clinical data to evaluate the predictive credibility of different components of the model.

One key feature of our model is the ability to translate *in vitro* assessments to clinical outcomes. Buprenorphine, which is known clinically to cause difficult-to-rescue respiratory depression,¹⁰ had the slowest dissociation rate from the opioid receptor in our study (**Table S2**). Interestingly, carfentanil, an ultrapotent fentanyl derivative considered of high concern in opioid overdose-associated death,³² had a dissociation rate almost as slow as buprenorphine (dissociation half-life ~47 minutes vs. 84 minutes, **Table S2**). Unlike buprenorphine, which is a partial opioid receptor agonist with a ceiling effect on respiratory depression,²⁸ carfentanil appears to be a full agonist with the capability of inducing apnea in animal studies.³³ To our knowledge, this is the first report that a full opioid receptor agonist possesses slow dissociation kinetics comparable to the partial agonist buprenorphine. In contrast, fentanyl,²⁶ as well as other fentanyl derivatives we tested that have been implicated in fatal community overdose cases, such as butyryl fentanyl,³⁴ furanyl fentanyl,³⁵ fluorobutyryl fentanyl,³⁶ and fluoroisobutyryl fentanyl,³⁷ had significantly faster dissociation rates from the opioid receptor (dissociation half-lives < 3 minutes; **Table S2**).

Another key feature of our modeling approach was the mechanistic representation of physiology, including the storage, metabolism, and exchange of gases (oxygen and carbon dioxide), ventilatory drives, and blood flow control. This allowed us to reproduce a wide range of clinical data probing the complex relationship between these components (see **Supplementary Materials**) and made it possible for the model to simulate opioid-induced respiratory depression as it would occur under real life conditions of patients breathing room air (poikilocapnic hypoxia). In contrast,

many published models ignored such physiological responses and were developed under conditions where end-tidal carbon dioxide partial pressure was fixed at an elevated level (isohypercapnic hypoxia), sometimes together with elevated end-tidal oxygen partial pressure.^{28,29,38} In addition, whereas models incorporating blood flow regulation were developed previously,^{16,17,30} they only accounted for what would happen in the initial minutes following ventilatory depression and predicted a continued increase in cardiac output and cerebral blood flow with prolonged respiratory depression. This is not physiological because continued severe hypoxia causes decompensation leading to decreased cardiac output and eventual cardiac arrest.^{18–20} Our model captured this mechanism to better reflect physiology after opioid overdose.

Being mechanistic in nature, our model can simulate many physiological outcomes during opioid-induced respiratory depression. In our initial simulation of opioid overdose and naloxone reversal in community settings, we focused on the end point of opioid-induced cardiac arrest. Opioid-associated out-of-hospital cardiac arrest is one of the leading causes of death associated with opioid overdose, and among all out-of-hospital cardiac arrests treated by emergency medical services, ~9% have been estimated to be due to opioid overdose.²¹ Although it is difficult to conduct clinical investigations studying opioid-induced cardiac arrest in humans, our mechanistic model and integrated approach provides a valuable tool for evaluating different opioid antagonists, along with doses and dosing strategies in this setting. Of note, patients who do not experience cardiac arrest may still have brain damage due to prolonged hypoxia. Our model simulates brain tissue oxygen partial pressure, and this could be used as an additional end point.

When simulating patients with opioid overdose, different patterns were observed. First, there were some differences in the physiological responses following overdose of different opioids. For example, compared with fentanyl, carfentanil takes longer to bind to the opioid receptor (K_{on}) and dissociate from the opioid receptor (K_{off}). This appears to contribute to ventilatory depression developing slightly more slowly after intravenous injection of carfentanil, compared to fentanyl; however, once ventilation decreases below 40% of baseline, the virtual patient has lower arterial oxygen partial pressure. Second, because carfentanil dissociates more slowly from the opioid receptor, it was more difficult to reverse respiratory depression compared with fentanyl, even when potency-normalized equivalent doses were given (see **Methods** section and **Figure 7**). Third, the more concentrated naloxone formulation rescued more patients than the lower concentration formulation with the same naloxone dose, which is consistent with it causing a faster rise in naloxone plasma concentration. This highlights how different naloxone products that have not been determined to be bioequivalent can have different pharmacokinetic properties that may lead to different outcomes.

There are limitations to the *in vitro-in silico* methodology developed in this work when it is applied to illicitly manufactured opioids without clinical pharmacokinetic data. First, similar to previous community-wide discussions about regulatory use of models,³⁹ the term “validation” is intended here as the evaluation of “how good is the model for a given prediction task” rather than of “how good is it as a representation of the real physiological system.”

Although some datapoints in the validation datasets have high variability, the ratio of mean values between model-predicted and observed datapoints across validation datasets has a median of 0.95 (interquartile range, 0.90–1.01), well below the previously recommended 2-fold range.²⁵

Second, not all parameters required to model a new opioid can be estimated through *in vitro* experiments. For example, pharmacokinetic parameters for many of the opioids tested in this study are unknown, and that is one of the reasons that, while we tested different fentanyl derivatives in our *in vitro* studies, only two (fentanyl and carfentanyl) were used in the initial overdose simulations. As obtaining human clinical pharmacokinetic data on many of these fentanyl derivatives that are not approved for human use is unlikely, we are exploring combining *in vitro* assays with physiologically-based pharmacokinetic modeling⁴⁰ to estimate their pharmacokinetic parameters for a more accurate assessment of naloxone dosage evaluation.

An additional limitation was that the pharmacodynamic parameters that govern the relationship between opioid receptor occupancy and the reduction of ventilatory drives may be opioid-specific but were assumed to be constant in this study. These pharmacodynamic parameters were estimated based on fentanyl clinical data during model calibration, and subsequently predicted clinical data for different fentanyl derivatives during model validation. The fact that the model predictions were highly similar to clinical data in the validation dataset (median ratio of predicted to measured values of 0.95 (interquartile range, 0.90–1.01)) suggests that the different fentanyl derivatives assessed may have similar pharmacodynamic parameters. Now that the validation step is completed, the model can be updated to have opioid-specific pharmacodynamic parameters based on clinical ventilation data when available.

Similarly, the *in vitro* submodel assumes simple competitive binding between opioids and naloxone on the opioid receptor, ignoring intricate mechanisms, such as G protein activation⁴¹ and multiple states of the opioid receptor.⁴² We adopted a “middle-out” approach⁴³ by keeping some submodels (such as the *in vitro*) more empirically derived and others (such as the physiological submodel) more mechanistic, with the aim of balancing biological reality and model complexity. Such a design dictates that the context of use of the model should be relevant to the validation procedure.⁴⁴ For example, our *in vitro* validation demonstrates the model’s capability of predicting the fraction of opioid-bound receptor in the presence of naloxone, and the pharmacodynamic validation demonstrates the possibility of translating such a fraction to respiratory depression-related clinical variables for fentanyl and its derivatives. However, opioids not structurally similar to fentanyl, or clinical end points related to other opioids’ effects like analgesia, might need more mechanistic *in vitro* simulations. For example, our current *in vitro* submodel, while able to capture the binding rate constants for buprenorphine, is not designed to recapitulate the partial agonist effect after receptor binding. This may be better described by a submodel with multiple states of the opioid receptor.⁴² The modular design of our model makes it straightforward to replace components of the model with alternative submodels.

In summary, we developed and validated a model that integrates pharmacokinetics, opioid receptor binding kinetics, pharmacodynamic effects on ventilation, and the physiological feedback

mechanisms involving lung gas exchange, blood gas transport, tissue oxygen, and carbon dioxide metabolism, as well as blood flow control. The blood flow components go beyond prior models to capture not only the compensatory response to hypoxemia, but also the subsequent decompensation that leads to cardiac arrest in the absence of a return of adequate respiration. Capturing this is critical to simulate the acute physiology of opioid overdose and assess opioid antagonist dosing to rescue patients prior to cardiac arrest. The *in vitro-in silico* methodology presented here is one of the first approaches proposed to assess naloxone dosing for newly emerging synthetic opioids with little clinical data, and has already begun to be used in the regulatory review of new naloxone product(s) and dosing strategies.^{45,46} This approach can be extended to cover other opioids and opioid antagonists (e.g., nalmefene⁴⁷) to aid in evaluating the effectiveness of different opioid antagonists or dosing strategies in a community setting.

SUPPORTING INFORMATION

Supplementary information accompanies this paper on the *Clinical Pharmacology & Therapeutics* website (www.cpt-journal.com).

ACKNOWLEDGMENTS

The authors would like to thank our colleagues for insightful discussions, especially Drs. Donna Volpe, Christopher Ellis, Lidiya Stavitskaya, and Rouse Rodney. This project was supported by the Research Participation Program at CDER, administered by the Oak Ridge Institute for Science and Education (ORISE) through an interagency agreement between the US Department of Energy and the FDA. This study used the computational resources of the High Performance Computing clusters at the Food and Drug Administration, Center for Devices and Radiological Health.

FUNDING

No funding was received for this work.

CONFLICT OF INTEREST

The authors declared no competing interests for this work.

AUTHOR CONTRIBUTIONS

Z.L. and J.M. wrote the manuscript. Z.L., D.G.S., and J.F. designed the research. J.M., A.E., A.J., K.W., T.S., and S.B. performed the research. A.C., J.Z., M.S., X.H., S.F.A., A.D., and E.O. analyzed the data.

DISCLOSURES

This article reflects the views of the authors and should not be construed to represent the FDA’s views or policies. As an Associate Editor for *Clinical Pharmacology & Therapeutics*, David G. Strauss was not involved in the review or decision process for this paper.

© 2022 The Authors. *Clinical Pharmacology & Therapeutics* © 2022 American Society for Clinical Pharmacology and Therapeutics. This article has been contributed to by U.S. Government employees and their work is in the public domain in the USA.

- Centers for Disease Control and Prevention. Drug overdose deaths <<https://www.cdc.gov/drugoverdose/deaths/index.html>> (2021).
- National Institute on Drug Abuse. Overdose death rates <<https://nida.nih.gov/drug-topics/trends-statistics/overdose-death-rates>> (2022).
- Scholl, L., Seth, P., Kariisa, M., Wilson, N. & Baldwin, G. Drug and opioid-involved overdose deaths—United States, 2013–2017. *MMWR Morb. Mortal. Wkly. Rep.* **67**, 1419–1427 (2018).
- The U.S. Department of Health and Human Services. What is the US opioid epidemic? <<https://www.hhs.gov/opioids/about-the-epidemic/index.html>> (2019).

5. Rzasla Lynn, R. & Galinkin, J.L. Naloxone dosage for opioid reversal: current evidence and clinical implications. *Ther. Adv. Drug Saf.* **9**, 63–88 (2018).
6. Lavonas, E.J. *et al.* Part 10: special circumstances of resuscitation: 2015 American Heart Association Guidelines Update for Cardiopulmonary Resuscitation and Emergency Cardiovascular Care. *Circulation* **132**, S501–S518 (2015).
7. USFDA. ZIMHI (naloxone hydrochloride injection) for intramuscular or subcutaneous use (FDA label) (2021).
8. USFDA. KLOXXADO (naloxone hydrochloride) nasal spray label <https://www.accessdata.fda.gov/drugsatfda_docs/label/2021/212045s000lbl.pdf> (2021).
9. USFDA. Summary minutes of the joint meeting of the anesthetic and analgesic drug products advisory committee and the drug safety and risk management advisory committee <<https://www.fda.gov/media/101166/download>> (2016).
10. Boom, M., Niesters, M., Sarton, E., Aarts, L., W. Smith, T. & Dahan, A. Non-analgesic effects of opioids: opioid-induced respiratory depression. *Curr. Pharm. Des.* **18**, 5994–6004 (2012).
11. Algera, M.H. *et al.* Tolerance to opioid-induced respiratory depression in chronic high-dose opioid users: a model-based comparison with opioid-naïve individuals. *Clin. Pharmacol. Ther.* **109**, 637–645 (2021).
12. Minto, C.F. *et al.* Influence of age and gender on the pharmacokinetics and pharmacodynamics of remifentanyl. I. Model Development. *Anesthesiology* **86**, 10–23 (1997).
13. Minkowski, C.P., Epstein, D., Frost, J.J. & Gorelick, D.A. Differential response to IV carfentanyl in chronic cocaine users and healthy controls. *Addict. Biol.* **17**, 149–155 (2012).
14. USFDA. Label for naloxone hydrochloride injection <<https://daily.med.nlm.nih.gov/dailymed/fda/fdaDrugXsl.cfm?setid=236349ef2cb5-47ca-a3a5-99534c3a4996&type=display>> (1988).
15. USFDA. Label for EVZIO Auto-Injector for intramuscular or subcutaneous use, 2 mg <https://www.accessdata.fda.gov/drugsatfda_docs/label/2016/209862lbl.pdf> (2016).
16. Ursino, M., Magosso, E. & Avanzolini, G. An integrated model of the human ventilatory control system: the response to hypercapnia. *Clin. Physiol.* **21**, 447–464 (2001).
17. Ursino, M., Magosso, E. & Avanzolini, G. An integrated model of the human ventilatory control system: the response to hypoxia. *Clin. Physiol.* **21**, 465–477 (2001).
18. Clowes, G.H. Jr., Hopkins, A.L. & Simeone, F.A. A comparison of the physiological effects of hypercapnia and hypoxia in the production of cardiac arrest. *Ann. Surg.* **142**, 446–459 (1955).
19. Elmer, J. *et al.* Effect of neuromonitor-guided titrated care on brain tissue hypoxia after opioid overdose cardiac arrest. *Resuscitation* **129**, 121–126 (2018).
20. Guedes, A., Aleman, M., Davis, E. & Tearney, C. Cardiovascular, respiratory and metabolic responses to apnea induced by atlanto-occipital intrathecal lidocaine injection in anesthetized horses. *Vet. Anaesth. Analg.* **43**, 590–598 (2016).
21. Dezfulian, C. *et al.* Opioid-associated out-of-hospital cardiac arrest: distinctive clinical features and implications for health care and public responses: a scientific statement from the American Heart Association. *Circulation* **143**, e836–e870 (2021).
22. Stoeckel, H. *et al.* Plasma fentanyl concentrations and the occurrence of respiratory depression in volunteers. *Br. J. Anaesth.* **54**, 1087–1095 (1982).
23. Mildh, L.H., Scheinin, H. & Kirvela, O.A. The concentration–effect relationship of the respiratory depressant effects of alfentanil and fentanyl. *Anesth. Analg.* **93**, 939–946 (2001).
24. Olofsen, E. *et al.* Modeling the non-steady state respiratory effects of remifentanyl in awake and propofol-sedated healthy volunteers. *Anesthesiology* **112**, 1382–1395 (2010).
25. Jones, H.M. *et al.* Physiologically based pharmacokinetic modeling in drug discovery and development: a pharmaceutical industry perspective. *Clin. Pharmacol. Ther.* **97**, 247–262 (2015).
26. National Drug Early Warning System. Unintentional fentanyl overdoses in New Hampshire: an NDEWS HotSpot analysis <<https://ndews.org/wordpress/files/2020/07/ndews-hotspot-unintentional-fentanyl-overdoses-in-new-hampshire-final-09-11-17.pdf>> (2017).
27. Voscopoulos, C.J., MacNabb, C.M., Freeman, J., Galvagno, S.M., Ladd, D. & George, E. Continuous noninvasive respiratory volume monitoring for the identification of patients at risk for opioid-induced respiratory depression and obstructive breathing patterns. *J. Trauma Acute Care Surg.* **77**, S208–S215 (2014).
28. Yassen, A. *et al.* Mechanism-based PK/PD modeling of the respiratory depressant effect of buprenorphine and fentanyl in healthy volunteers. *Clin. Pharmacol. Ther.* **81**, 50–58 (2007).
29. Yassen, A. *et al.* Mechanism-based pharmacokinetic–pharmacodynamic modelling of the reversal of buprenorphine-induced respiratory depression by naloxone. *Clin Pharmacokinet* **46**, 965–980 (2007).
30. Magosso, E., Ursino, M. & van Oostrom, J.H. Opioid-induced respiratory depression: a mathematical model for fentanyl. *IEEE Trans. Biomed. Eng.* **51**, 1115–1128 (2004).
31. Moss, R.B. *et al.* Higher naloxone dosing in a quantitative systems pharmacology model that predicts naloxone-fentanyl competition at the opioid mu receptor level. *PLoS One* **15**, e0234683 (2020).
32. Cole, J.B. & Nelson, L.S. Controversies and carfentanyl: we have much to learn about the present state of opioid poisoning. *Am. J. Emerg. Med.* **35**, 1743–1745 (2017).
33. Port, J.D., Stanley, T.H., Steffey, E.P., Pace, N.L., Henrickson, R. & McJames, S.W. Intravenous carfentanyl in the dog and rhesus monkey. *Anesthesiology* **61**, A378 (1984).
34. Poklis, J. *et al.* Two fatal intoxications involving butyryl fentanyl. *J. Anal. Toxicol.* **40**, 703–708 (2016).
35. Papsun, D., Hawes, A., Mohr, A.L.A., Friscia, M. & Logan, B.K. Case series of novel illicit opioid-related deaths. *Acad. Forensic Pathol.* **7**, 477–486 (2017).
36. Rojkiewicz, M., Majchrzak, M., Celiński, R., Kuś, P. & Sajewicz, M. Identification and physicochemical characterization of 4-fluorobutyrylfentanyl (1-((4-fluorophenyl)(1-phenethylpiperidin-4-yl)amino)butan-1-one, 4-FBF) in seized materials and post-mortem biological samples. *Drug Test Anal.* **9**, 405–414 (2017).
37. World Health Organization. 4-Fluorobutyrylfentanyl (4-FIBF) review report <https://www.who.int/medicines/access/controlled-substances/Critical_Review_4FIBF.pdf> (2017).
38. Babenco, H.D., Conard, P.F. & Gross, J.B. The pharmacodynamic effect of a remifentanyl bolus on ventilatory control. *Anesthesiology* **92**, 393–398 (2000).
39. Li, Z. *et al.* General principles for the validation of proarrhythmia risk prediction models: an extension of the CiPA in silico strategy. *Clin. Pharmacol. Ther.* **107**, 102–111 (2020).
40. Feasel, M., The use of in vitro and in silico technologies for predicting human pharmacology and toxicology of carfentanyl (2017).
41. Gillis, A. *et al.* Low intrinsic efficacy for G protein activation can explain the improved side effect profiles of new opioid agonists. *Sci. Signal* **13**, eaaz3140 (2020).
42. Sadee, W., Oberdick, J. & Wang, Z. Biased opioid antagonists as modulators of opioid dependence: opportunities to improve pain therapy and opioid use management. *Molecules* **25**, 4163 (2020).
43. Tsamandouras, N., Rostami-Hodjegan, A. & Aarons, L. Combining the ‘bottom up’ and ‘top down’ approaches in pharmacokinetic modelling: fitting PBPK models to observed clinical data. *Br. J. Clin. Pharmacol.* **79**, 48–55 (2015).
44. V&V40. Assessing credibility of computational modeling and simulation results through verification and validation: application to medical devices (2018).
45. USFDA. Clinical review for NDA215457 (Naloxone Auto-Injector 10 mg) <https://www.accessdata.fda.gov/drugsatfda_docs/nda/2022/215457Orig1s000MedR.pdf> (2022).

46. USFDA. Clinical Pharmacology Review for NDA215457 (Naloxone Auto-Injector 10mg) <https://www.accessdata.fda.gov/drugs_atfda_docs/nda/2022/215457Orig1s000ClinPharmR.pdf> (2022).
47. Krieter, P., Gyaw, S., Crystal, R. & Skolnick, P. Fighting fire with fire: development of intranasal nalmefene to treat synthetic opioid overdose. *J. Pharmacol. Exp. Ther.* **371**, 409–415 (2019).
48. Duffin, J., Hare, G.M.T. & Fisher, J.A. A mathematical model of cerebral blood flow control in anaemia and hypoxia. *J. Physiol.* **598**, 717–730 (2020).
49. Battisti-Charbonney, A., Fisher, J. & Duffin, J. The cerebrovascular response to carbon dioxide in humans. *J. Physiol.* **589**, 3039–3048 (2011).
50. Mardimae, A. et al. The interaction of carbon dioxide and hypoxia in the control of cerebral blood flow. *Pflugers Arch.* **464**, 345–351 (2012).
51. American College of Emergency Physicians online publication: Avoid airway catastrophes on the extremes of minute ventilation <<https://www.acepnow.com/article/avoid-airway-catastrophes-extremes-minute-ventilation/>> (2015).